# Chapter 3

# Assembly and Integration of *SUIT*

*'Where there is a loose washer, there has to be a loose nut.'*

— Richard Preston, *First Light.*

The assembly and integration of a space telescope is a crucial step as the instrument has to survive extreme levels of vibration, shock, and thermal gradients during the lift-off and in space. The integration should be reliable to survive such extreme conditions and not cause the optical components to move or get damaged. The integration of *SUIT* involves the optical alignment, followed by the integration of all mechanical parts, along with the implementation of payload heaters, thermal sensors, and CCD cooling setup.

In this chapter, section 3.1 presents the optical alignment procedure and results of *SUIT*. Section 3.2 explains the mounting procedure for the thermal filter assembly at the front aperture of *SUIT*. Sections 3.3 and 3.4 explain the implementation of thermal components, followed the satellite mounting process for *SUIT*.

## 3.1 Optical Alignment

Optical alignment refers to the alignment of all the optical components, followed by verification of the instrument wavefront to ensure good image quality.

### 3.1.1 Preparation

The alignment process is started by assigning a reference mirror at one end of the lab. This mirror will serve as the optical alignment reference throughout the alignment process. Therefore, the mirror is locked in place and is not touched at all throughout the alignment process. Generally, the mirror is placed such that its optical axis is perpendicular to the gravity vector. A theodolite (Leica TM 6100A) is used for performing optical alignments. This theodolite has autocollimation capabilities and is subsequently referred to as autocollimator in the text. The autocollimator axis is made perpendicular to the gravity vector, and the reference mirror is adjusted to achieve autocollimation.

The next step is to ensure the flatness and perpendicularity of the optical tabletop with respect to the gravity vector. The autocollimator is made perpendicular to the gravity vector with $0.1''$ accuracy. *SUIT* has six legs that mount the optical bench to the satellite deck, and also to the optical table. The footprints of these legs are identified on the table. Due to the non-planarity of the table surface, some of these points might be depressed, and some might be elevated. An optical cross-wire target is placed at the payload footprint location with the least depression. The height of the optical cross-wire target is set to coincide with the theodolite cross-wire. This target is moved to the other footprint locations on the table. The target appears depressed with respect to the theodolite cross wire at the other locations. The height is adjusted to match the theodolite axis by adding shims underneath the target stand. This gives the number of shims required to compensate for various levels of depression at the 6 footprint locations of the *SUIT* optical bench within an accuracy of $25\mu m$. The six payload pods are mounted on the table at their identified footprint locations. The optical bench is mounted on the legs with appropriate shims in between to account for the non-planarity and tilt of the table with respect to the reference mirror. This makes the payload bench perpendicular to the gravity vector.

Next, the *SUIT* optical bench is mounted on the pods. The orientation of the optical bench is such that the primary mirror axis should be aligned with the axis of the reference mirror. The planarity of the optical bench is also inspected. This is to identify any unevenness from one point to another among

the optical bench mounting locations. Irregularity in the flatness can lead to a series of additive errors in each optical sub-assembly while performing the optical alignment. The same method is used to verify the planarity of the optical bench at various sub-assembly mounting locations. The largest difference noticed between the highest and lowest points on the bench is measured to be 150 $\mu m$, which can be compensated by using appropriate shims while the sub-assemblies are mounted.

### 3.1.2 Mirror Alignment

The alignment of the *SUIT* mirrors is the most crucial task in the alignment process, as this determines the optical performance of the payload. Figure 3.2 shows the primary and secondary mirror assemblies. The first step is to identify the detector plane and the on-axis focus position of the telescope. For this, a mechanical model of the *SUIT* CCD is used. The mechanical CCD has similar dimensions to the *SUIT* CCD; however, it is made of a block of aluminum. The mechanical CCD is mounted on the detector housing assembly (DHA), which is used to position the CCD at the correct location on the optical bench. A cross mark is made across diagonal corners of the mechanical CCD. This is used as a reference to determine the exact position of the CCD center within $\pm 50 \mu m$, which translates to $\pm 2.9''$. An optical needle is used to spatially mark the X-Y-Z location of the CCD center. The position of the pointer needle along the optical axis is set keeping in mind the offset in the focal position due to the absence of the science filters and field corrector lens.

The secondary mirror (M2) to DHA arm is at an angle of 2.64° with respect to the incident direction of sunlight, which is defined by the reference mirror. The autocollimator is aligned with the reference mirror, and a 6-inch flat mirror is introduced in front of it. The tilt of this mirror is adjusted to achieve autocollimation. Now, the autocollimator is rotated by 2.64° towards the side of the primary mirror (M1), and the mirror tilt is adjusted to achieve autocollimation again.

A Fizeau interferometer is placed at a distance of 2500 mm from the focal plane of *SUIT*. The interferometer is pointed towards the 6-inch mirror set at an angle of 2.64°, and its tilt is adjusted to achieve null fringes. Now, the

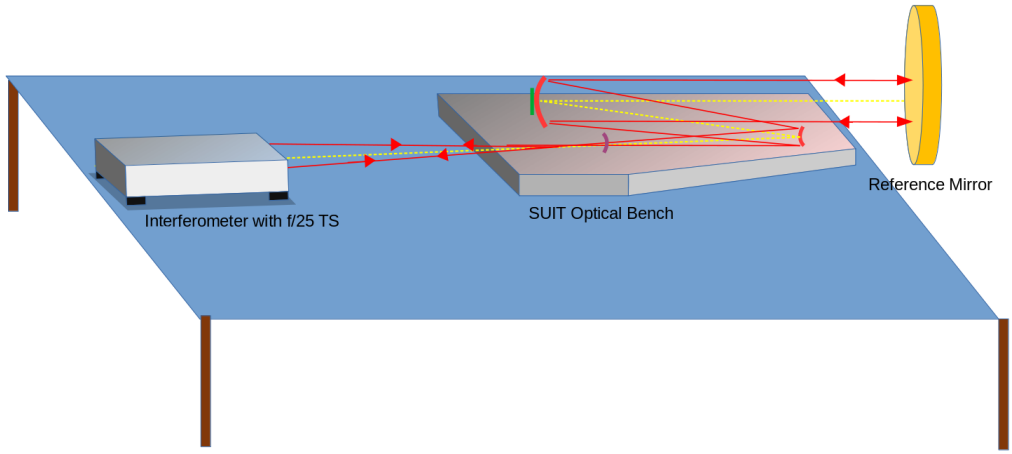


**Figure 3.1:** Schematic diagram of the setup for performing the optical alignment of *SUIT*. A fizeau interferometer is used with a f/25 transmissioin sphere to focus light at the focal plane of the telescope. This light is retroreflected by the reference mirror. The wavefront at the focal plane of the telescope is used to determine the optical quality and nature of aberrations.

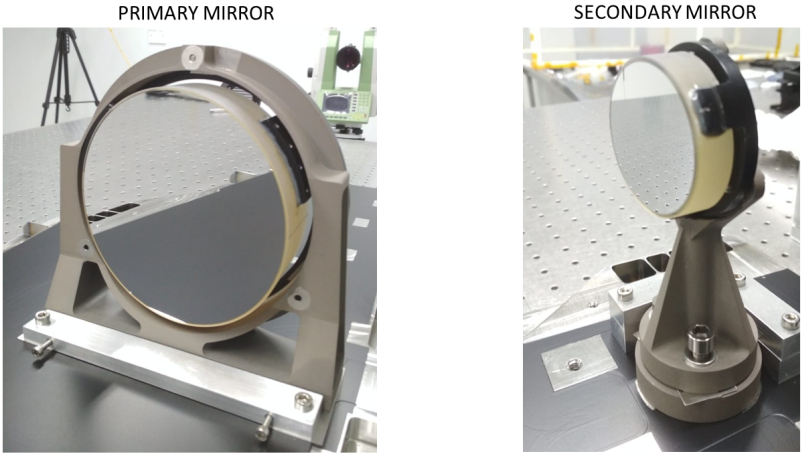


**Figure 3.2:** Flight model of the Primary (left) and the secondary (right) mirror assemblies [34].

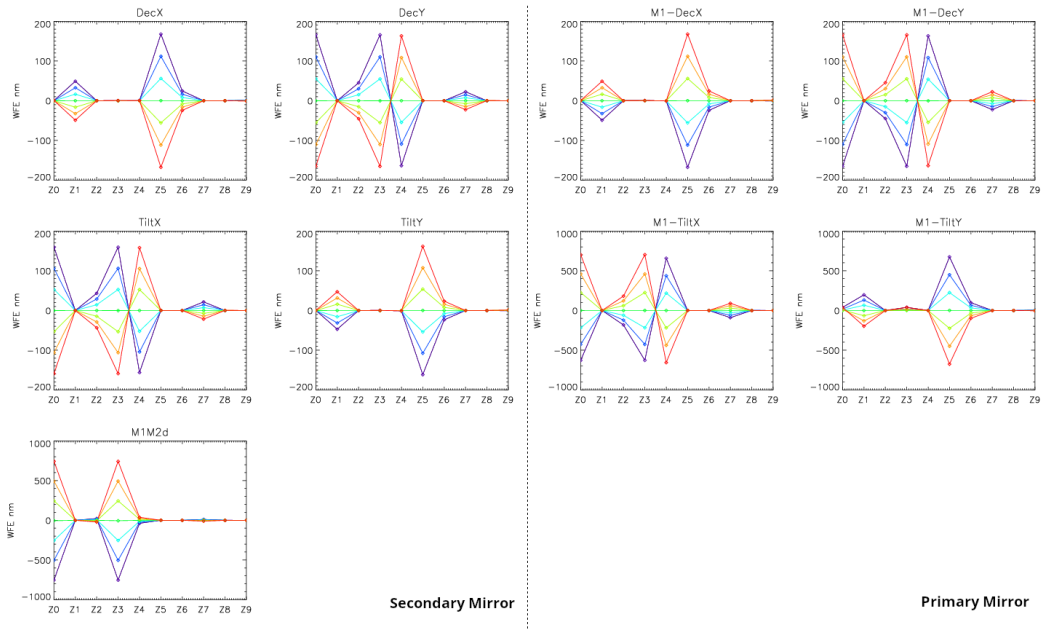


**Figure 3.3:** Contribution of Zernike coefficients (Z#) to wavefront error (WFE) with 33 micron steps of de-center and 2′ steps of tilt for the primary and secondary mirrors, while keeping every other component at their nominal positions.

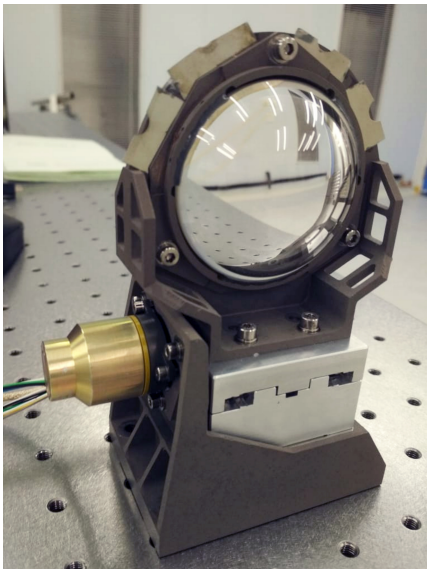

**Figure 3.4:** Flight model of field corrector lens assembly.

| Aberration | *SUIT* payload (nm) | Collimator (nm) |
|---|---|---|
| **RMS** | 34 | 41.4 |
| **PVr** | 196.4 | 210.3 |
| **Power** | 25 | -4.4 |
| **Astig X** | -32.7 | 36.7 |
| **Astig Y** | 22.8 | 0.88 |
| **Coma X** | -30.8 | -63.3 |
| **Coma Y** | -9.9 | 28.8 |
| **Primary Spherical** | -19.8 | -18.8 |
| **Trefoil X** | -13.9 | -40.4 |
| **Trefoil Y** | -17.3 | -19.3 |

**Table 3.1::** Zernike coefficients representing the extent of optical aberrations of the *SUIT* payload and collimator. The red peaks and blue valleys show the extent of deviation from the ideal plane wavefront.

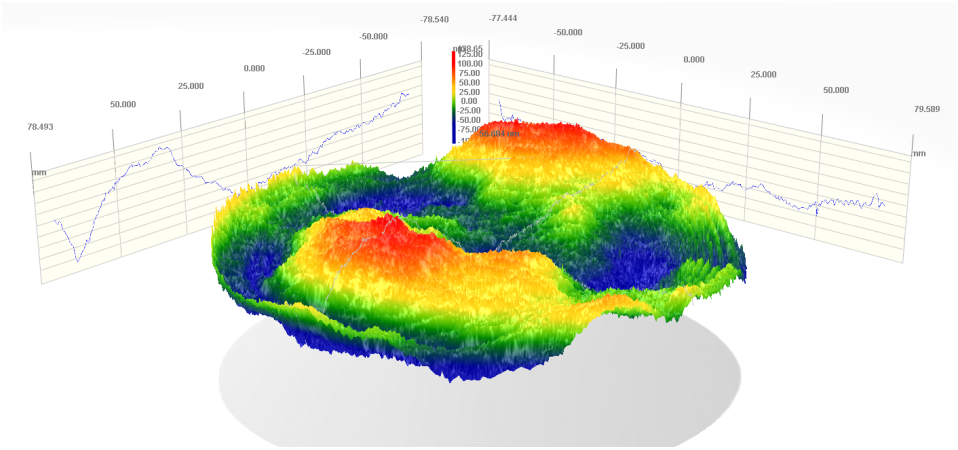


**Figure 3.5:** Final wavefront map of *SUIT* after optical alignment of M1, M2 and FCLA. The red peaks and blue valleys represent the deviation from the ideal plane wavefront. The RMS of the wavefront surface is measured to be 34 nm.

interferometer is at an angle of 2.64° with respect to the direction of incident sunlight, same as the axis of the secondary mirror to DHA arm. Now, the interferometer has to be shifted laterally, while maintaining a fixed distance and angle from the focal plane. A flat mirror is mounted behind the interferometer, and the autocollimator is aligned with it. This is to ensure the tilt of the interferometer does not change while it is laterally shifted in vertical or horizontal directions.

Once placed correctly, a 100 mm f/25 transmission sphere is mounted on the interferometer to focus the beam at the location of the DHA center, defined by the optical needle. The interferometer height and lateral position are adjusted with respect to the optical needle, keeping the interferometer tilt unchanged with feedback from the theodolite. A small plane mirror is placed at the focal plane with reference from the optical needle. The mirror tilt is adjusted to retroreflect the beam back to the interferometer. Circular fringes might appear, which is an indication of improper positioning of the interferometer along the chief ray (Z-Axis). The position of the interferometer is adjusted accordingly to get null fringes. The small mirror is removed, and the X-Y position of the interferometer beam is checked for any offsets with respect to the position, which would be the center of the CCD. If offsets arise, this step is repeated, and corrections are made iteratively.

The next step involves mounting the primary and secondary mirrors. However, before physically mounting the mirrors, the nature of variation in optical properties with the movement of each optical component is simulated in Ze-

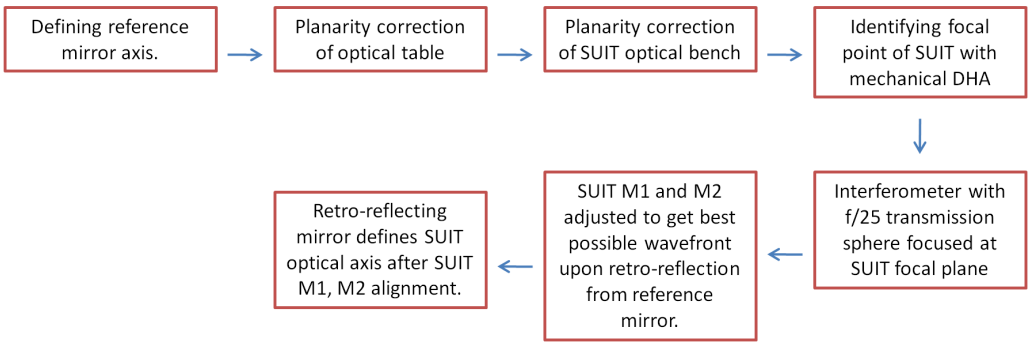


**Figure 3.6:** Flow chart summarizing the sequence of activities undertaken for optical alignment and defining the optical axis of *SUIT*.

max. Each individual optical component is tilted and decentered about all three axes in the Zemax model while keeping others at their optimal position.

The change in the Zernike coefficients of *SUIT* is simulated with each movement step of individual optical components. This gives an idea of the trend for every type of aberration with the movement of each optical element, as seen in Figure 3.3. The guidance obtained helps to determine the required movement on the mirrors so that the net aberration of the complete telescope system can be minimized.

The optical property of the telescope is determined by the reproduced wavefront at the telescope. The extent of optical aberration is determined by the deviation of the wavefront from an ideal flat surface at the focal plane of the telescope. This is if the wavefront at the focal plane were collimated. The reproduced wavefront is fitted with a 35-term 2D polynomial called Zernike polynomial. Each component of the polynomial is orthogonal, and the coefficient of each component is representative of a specific type of Siedel aberration such as Astigmatism, Coma, Trefoil, etc., in the telescope optics. The RMS height of various peaks and valleys of the wavefront gives the telescope's overall performance.

The primary and secondary mirror assemblies are now mounted on the optical bench. Guide blocks are attached together with the mirrors to accurately adjust the mirror position and tip-tilt. The Field-Corrector Lens Assembly (FCLA) is placed on the optical path after the mirrors are placed (Figure 3.4). Light from the Fizeau interferometer is focused at the point where the chief-ray of the telescope hits the focal plane as illustrated in Figure 3.1. The f-number of the light from the interferometer is the same as that for the telescope. So, the light tightly fills M1 after reflection from M2. This light is retroreflected back to the interferometer by the reference mirror. The interferogram of the return beam is used to generate a 3D model of the telescope wavefront and determine the Zernike coefficients. Interferograms are recorded after each actuation of each individual component, and the Zernike coefficients are monitored. Once the mirror positions are set, the mirror mounts are carefully shimmed and torqued to arrest their movement. Care is taken that the mirrors do not move while doing so. The final wavefront of *SUIT* is shown in Figure 3.5, and the final set of Zernike coefficients, as in Table 3.1, defines the

optical quality of *SUIT*. The RMS of the wavefront is 34 nm, corresponding to $\lambda/8.8$ at 300 nm, signifying good optical alignment. The reference mirror used for retro-reflecting the interferometer light now defines the optical axis of the payload

Similar steps are followed for aligning the optics of the *SUIT* flight spare model. The mirrors on the flight spare are also aligned to have comparable optical performance as the *SUIT* flight model. This flight spare is later repurposed as a NUV collimator for *SUIT*'s calibration experiments described in Chapters 4 and 5.

### 3.1.3 Alignment Cube

An alignment cube is a carefully manufactured cube, with five polished reflective sides which are perpendicular to their adjacent sides to a high level of accuracy. An alignment cube is used as an optical reference for aligning optical components or instruments. In *SUIT*, we use an alignment cube as a reference for the instrument optical axis. This is necessary to align the telescope with the satellite axis.

After the optical alignment of *SUIT*, the DHA with the mechanical CCD is mounted on the payload bench to identify the center of the payload focal plane. Collimated parallel beam from the interferometer is made incident at the entrance aperture of *SUIT* as illustrated in Figure 3.8. The tip-tilt of the interferometer is adjusted such that the beam converges at the center of the

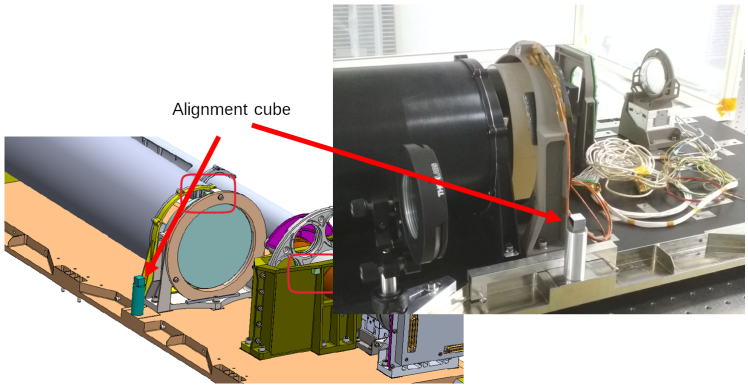


**Figure 3.7:** The position of the alignment cube on the *SUIT* payload. The alignment cube sits on a cylindrical stand, next to the primary mirror (M1).

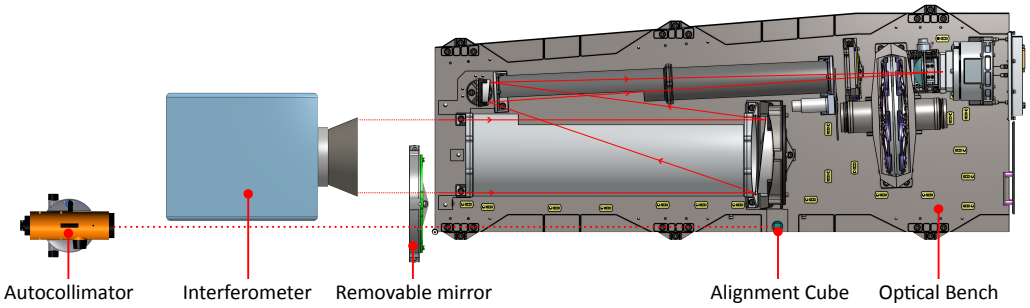


**Figure 3.8:** Schematic diagram of the optical setup used to find the *SUIT* optical axis and for measuring the angular offsets with the alignment cube axis.

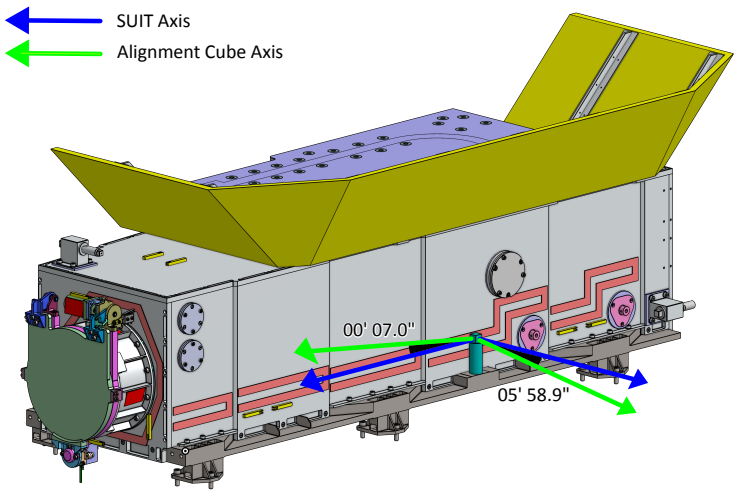


**Figure 3.9:** Angular offset of the alignment cube axis with the *SUIT* axes. The *SUIT* axes (blue arrow) and alignment cube axes (green arrow) are represented as a schematic on the faces of the alignment cube.

| **Source of uncertainty** | **Uncertainty** |
|---|---|
| DHA positioning (horizontal) | $< \pm 5.8''$ |
| DHA positioning (vertical) | $< \pm 2.9''$ |
| Theodolite orientation and Mirror coalignment | $< \pm 7.5''$ |
| Max. total uncertainty $\left(\sqrt{x_1^2 + x_2^2 + ... + x_n^2}\right)$ | $< \pm 9.9''$ |

**Table 3.2::** List of uncertainties in co-aligning the alignment cube with *SUIT* optical axis.

mechanical CCD. This ensures that the interferometer axis is parallel to the optical axis of the telescope. A big mirror (6-inch diameter) is placed in the beam path of the interferometer. The tip-tilt of the mirror is adjusted such that null fringes are achieved in the mirror's interferogram, ensuring the mirror is aligned with the interferometer axis. This allows the mirror to be aligned with the optical axis of the interferometer and the telescope.

The alignment cube is glued on a cylindrical stand with 3M-Scotch Weld EC2216 bonding compound and is left to cure for 24 hrs at room temperature. After curing, the alignment cube with its stand is placed on the payload at its designated position, beside the primary mirror on the -ve pitch side, as illustrated in Figure 3.7. The alignment cube's axis is checked with the autocollimator. Firstly, the autocollimator is adjusted so that it is aligned with the mirror and the instrument's optical axis. The lateral position of the autocollimator is also adjusted so that, the alignment cube falls in its line of sight. The mirror is removed, and the alignment cube is rotated such that the best possible autocollimation is achieved with the theodolite. A height gauge is used to apply pressure from the top of the alignment cube and stand to arrest any movement. 3M Scotch-Weld EC2216 bonding compound is used to bond the alignment cube stand onto the payload bench and is left to cure for 24 hours at room temperature and pressure. After curing, the alignment cube axis is verified by repeating the procedure above. The angular offset of the alignment cube axis with *SUIT*'s optical axis is measured with the autocollimator and noted. This offset needs to be considered while aligning the payload on the satellite.

The uncertainties in the axis of the alignment cube can arise from- deviant positioning of the mechanical CCD while retracing the optical axis, faulty positioning of the reference mirror, and measurement error of the autocollimator. The play of the DHA on the payload bench is $< \pm 0.1\ mm$. This corresponds to $< \pm 5.8''$ uncertainty in the determination of the optical axis horizontally. The uncertainty in the vertical positioning of the DHA is $< 0.05\ mm$, corresponding to $< 2.9''$. The uncertainty in theodolite and reference mirror orientation is $< \pm 7.5''$. Thus, the maximum overall uncertainty in retracing the *SUIT* optical axis with the theodolite to align the alignment cube is $< \pm 9.9''$. An overall account is represented in Table 3.2.

After 24 hours of recommended bond curing, the offset of the alignment cube axis with respect to the *SUIT* optical axis is $+5'58.9''$ about pitch when viewed from the thermal filter side, and + 0.7 $''$ about roll when viewed from the top, as illustrated in Figure 3.9. The comparatively low offset in orientation about the roll axis is due to the mechanical interface of the alignment cube stand and the payload bench. The positioning of the cube can be set accurately about the roll axis by rotating the alignment cube stand. However, the offsets in the pitch axis cannot be corrected as this would call for vertically tilting the alignment cube stand, which is cumbersome and might compromise the mechanical rigidity of the bonding with the *SUIT* optical bench.

### 3.1.4 CCD alignment

The alignment of the CCD is of utmost importance, as this defines the position of the image on the CCD. This is also crucial, as any unwanted tilt can cause some portions of the CCD to fall out of the telescope's depth of focus, causing some portions of the image to appear blurred. The CCD is held by the detector housing assembly, along with the necessary mechanical and thermal implementation required for the proper functioning of the detector. The CCD surface should be at the focal plane of the telescope. It is also ensured that any relative tilt between the focal plane and the CCD plane should be within tolerable limits of the telescope's depth of focus.

The autocollimator is aligned along the secondary mirror axis of the telescope after they have been aligned. A plane mirror is placed on a calibrated rotation stage and placed on the *SUIT* optical bench. The tip-tilt of the mirror is adjusted to achieve autocollimation. This mirror is rotated by 90 degrees using the rotation stage. The autocollimator is shifted by 90 degrees and taken to the +pitch side of *SUIT*, where it is autocollimated with this mirror. Now, the mirror is rotated by 45 degrees, such that the CCD surface can be seen through the autocollimator. The CCD surface is highly reflective in visible light. This is used to our advantage as we adjust the tip-tilt of the detector housing assembly with the help of shims under the mount to achieve autocollimation. This leads to the CCD being aligned with the M2 axis. Figure 3.10 shows a CAD representation and a photograph of the assembled DHA.

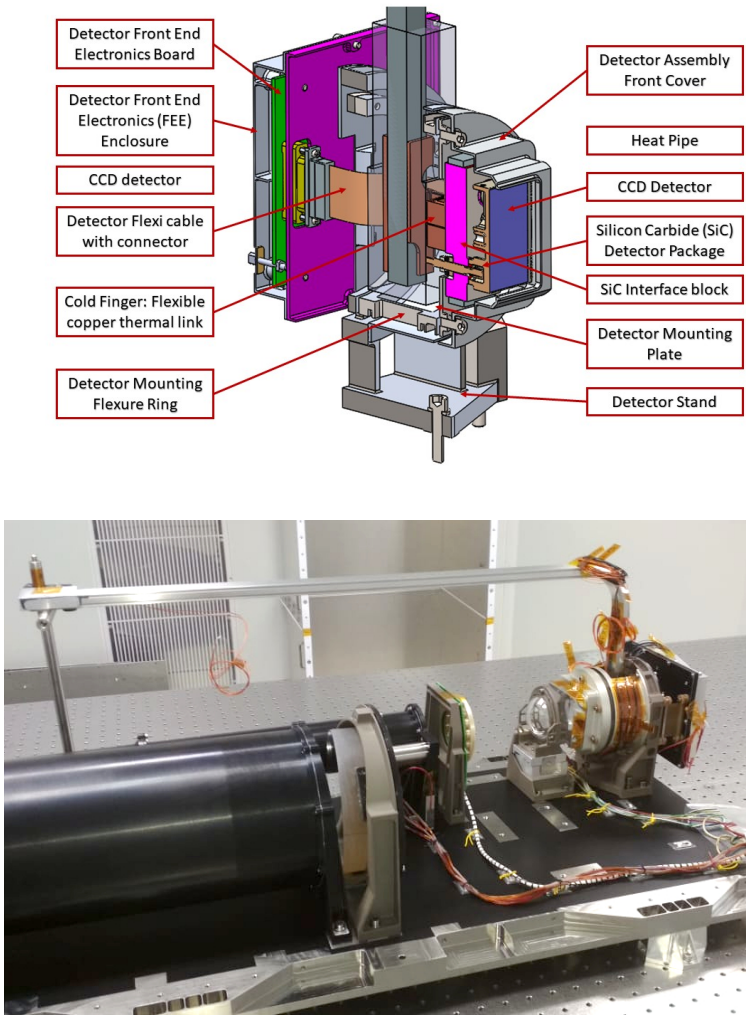


**Figure 3.10:** Top: A CAD representation (sectioned view) of the detector Assembly showing the mounting scheme and cooling chain for the detector. Bottom: Detector Assembly and heat pipe mounted on *SUIT*[34].

## 3.2 Thermal filter mounting

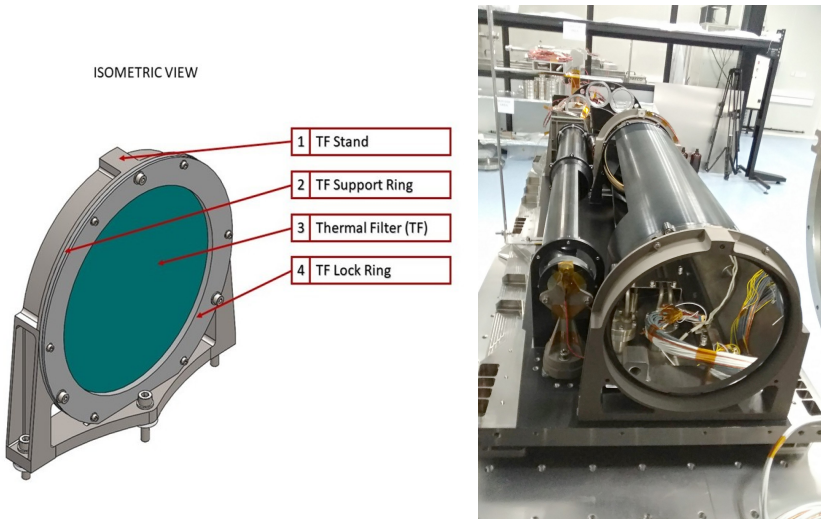


**Figure 3.11:** Isometric view (left) and actual photo (right) of the thermal filter assembly mounted on the *SUIT* optical bench [34].

The thermal filter assembly (TFA) [41, 42] sits at the front aperture of *SUIT*. Therefore, any light entering the telescope has to first pass through the TFA. Therefore, it is very necessary to ensure the optical quality of the TFA.

Light from the interferometer is fed into *SUIT* along the optical axis as described in section 3.1.3. The thermal filter is then placed on the optical bench, and the reflected wavefront from the front surface of the thermal filter is monitored in the interferometer. Ideally, the transmitted wavefront is monitored for such transmission optics. However, because of the high reflectance of the thermal filter, the reflected wavefront is used to monitor the shape of the glass surface. The thermal filter is very sensitive to mechanical stresses. So, any uneven stress introduced while mounting the TFA on the optical bench can cause severe changes in the reflected wavefront. Shims of appropriate thickness are used at the mounting points while tightening the bolts. The bolts are torqued gradually to the recommended value while actively monitoring the wavefront to ensure we do not introduce any distortions to the thermal filter while mounting. Figure 3.11 shows the CAD diagram and a photo of the assembled TFA.

## 3.3 Mounting of non-optical components

After the optical alignment and integration of the flight model of *SUIT*, the instrument is finally assembled for space qualification tests. The primary and secondary baffles are integrated, followed by the LED mount, filter wheel assembly, and the vane shutter mechanism. A field-of-view test is performed in the lab as mentioned in section 5.1.1. This is to ensure no part of the beam reaching the CCD is obstructed by any of these components.

The wires for the heaters, thermal sensors, and accelerometers are securely routed along the optical bench. This step is very crucial, as any unnoticed damage to the wires, or improper fastening could lead to compromised performance, if not complete failure of the payload. The cover panels are closed, and the heat pipe is secured to the top cover panel. The radiator plate is mounted to the CCD heat pipe and an iridium film is used between the heat pipe and the radiator plate to improve thermal conduction.

## 3.4 Satellite Mounting

*SUIT* and *VELC* are optical payloads on board Aditya-L1. Both the payloads have to be aligned accurately within a margin of $2'$ for observing the Sun simultaneously. Misalignment of either payload can lead to one of them not being pointed at the Sun while the other is. The optical axis of the *SUIT* payload is defined by its alignment cube as mentioned in section 3.1.3. The magnitude and direction of the axis offset between the *SUIT* optical axis and the cube is measured accurately while mounting the cube. This is used to co-align *VELC* with the *SUIT* payload.

*VELC* and *SUIT* are mounted on the top Aditya-L1. *VELC* is a heavy

| **Optical Axis of *SUIT*** | **Rotation about Roll** | **Rotation about Pitch** |
|---|---|---|
| Before Correction | $00°06'0''$ | $00°02'02''$ |
| After Correction | $-00°01'08''$ | $00°01'56''$ |

**Table 3.3::** Offset of *SUIT* Optical axis with respect to VELC optical axis before and after alignment correction.

payload, weighing $\approx$ 200 kg. Therefore, it is easier to make fine adjustments on *SUIT* for matching payload axes. Upon mounting, the axes of the two payloads are verified by autocollimation. After mounting *SUIT*, the optical axes the two instruments are seen to have an offset of $> 6'$. This is much larger than the design tolerance of $2'$. To make necessary corrections, the pods mounting *SUIT* to the satellite deck are re-fabricated such that the *SUIT* axis misalignment with *VELC* is $< 2'$. The pre and post-correction optical axis offsets of *SUIT* with respect to *VELC* are tabulated in Table 3.3.